ARCTIC
VOL. 61, NO. 4 (DECEMBER 2008) P. 381–394

Recent (1986–2006) Vegetation-Specific NDVI Trends in Northern Canada from Satellite Data

IAN OLTHOF,[1,2] DARREN POULIOT,[1] RASIM LATIFOVIC[1] and WENJUN CHEN[1]

(*Received 4 September 2007; accepted in revised form 8 January 2008*)

ABSTRACT. Recent northern vegetation changes caused by climate warming have been well documented, using experimental plot warming to examine vegetation-specific changes and satellite image data to examine overall trends. Previous remote sensing efforts have employed the Normalized Difference Vegetation Index (NDVI) from AVHRR, whose 1 km to 8 km pixel size is too large for examination of broad scale vegetation-specific responses because of mixing within the pixel footprint. In this paper, we reconcile differences between field- and remote sensing-based approaches by using both medium-resolution (30 m) and coarse-resolution (1 km) data to study 20 years of vegetation-specific responses to northern climate warming (1986 to 2006). Trends are compared among vegetation communities from two separate Landsat classifications in Canada's eastern and western forest-tundra transition zone, as well as a 1 km AVHRR database recently developed over Canada. A comparison of absolute trends among mapped vegetation communities revealed lichen-dominated communities consistently exhibiting lower trends than those dominated by vascular plants, with both exhibiting increasing NDVI. Our results and those obtained from experimental warming suggest that the magnitude difference in NDVI increase between lichen and vascular vegetation is related to increasing vigor and biomass of vascular vegetation, in contrast to physiological impairment of lichen due to the short-term secondary effect of temperature on moisture. In the longer term, succession from lichen to vascular is likely responsible for the small observed NDVI increase over lichen-dominated regions. The fact that both Landsat and AVHRR exhibited similar relative vegetation-specific trends in NDVI suggests that this phenomenon may be widespread in the North.

Key words: northern, vegetation, community, lichen, vascular, remote sensing, Landsat, AVHRR, NDVI, trends

RÉSUMÉ. Ces derniers temps, les changements sur la végétation dans le Nord causés par le réchauffement climatique ont été bien documentés grâce à une parcelle expérimentale faisant l'objet d'un réchauffement qui permet d'examiner les changements propres à la végétation, ainsi que grâce à des données et images obtenues par satellite permettant d'examiner les tendances générales. Les travaux de télédétection antérieurs recouraient à l'indice d'activité végétale obtenu à partir d'un radiomètre perfectionné à très haute résolution (AVHRR), dont la taille de pixel de 1 km à 8 km est trop grande pour permettre l'examen des réactions à grande échelle de la végétation en raison du mélangeage dans la zone de couverture des pixels. Dans cette communication, nous faisons le rapprochement des différences entre les méthodes de prélèvement de données sur le terrain et les méthodes de prélèvement des données par télédétection en recourant à des données à moyenne résolution (30 m) et à des données à résolution grossière (1 km) dans le but d'étudier les réactions de la végétation échelonnées sur 20 ans dans le cadre du réchauffement climatique dans le Nord (de 1986 à 2006). Les tendances sont comparées entre les diverses communautés végétales à partir de deux classifications Landsat distinctes dans la zone de transition forêt-toundra de l'est et de l'ouest du Canada, ainsi qu'à partir d'une banque de données prélevées au Canada à l'aide d'un radiomètre perfectionné à très haute résolution de 1 km récemment mis au point. La comparaison des tendances absolues parmi les communautés végétales mappées a révélé des communautés dominées par le lichen affichant constamment des tendances moins élevées que les communautés dominées par les plantes vasculaires, toutes deux présentant un indice d'activité végétale accrue. Nos résultats et ceux obtenus dans le cadre du réchauffement expérimental laissent croire que la différence de magnitude en ce qui a trait à l'accroissement de l'indice d'activité végétale entre la végétation de lichen et la végétation vasculaire se rapporte à l'accroissement de la vigueur et de la biomasse de la végétation vasculaire, par contraste avec l'altération physiologique du lichen attribuable à l'effet secondaire à court terme de la température sur l'humidité. À plus long terme, la succession du lichen aux plantes vasculaires est vraisemblablement responsable des petites augmentations observées au titre de l'indice d'activité végétale dans les régions dominées par le lichen. Le fait que le Landsat et l'AVHRR aient tous deux permis de dénoter des tendances relatives semblables du point de vue de la végétation et de l'indice d'activité végétale laisse entendre que ce phénomène peut être étendu dans le Nord.

Mots clés : nord, végétation, communauté, lichen, vasculaire, télédétection, Landsat, AVHRR, indice d'activité végétale, tendances

Traduit pour la revue *Arctic* par Nicole Giguère.

[1] Applications Division, Canada Centre for Remote Sensing, 588 Booth Street, Ottawa, Ontario K1A 0Y7, Canada
[2] Corresponding author: iolthof@nrcan.gc.ca

INTRODUCTION

Climate warming is expected to continue to be greatest during the 21st century at northern high latitudes, according to General Circulation Model (GCM) predictions (IPCC, 2007). Northern environments have already experienced significant vegetation changes due to climate warming (Myneni et al., 1997; Stow et al., 2004; Goetz et al., 2005; Pouliot et al., in press). In general, these changes are expected to alter northern ecosystem properties such as surface albedo, soil thermodynamics, hydrology, and earth-atmosphere interactions (ACIA, 2004). Northern vegetation also provides critical habitat for species such as caribou in northwestern Canada and Alaska. In this region, the Porcupine caribou herd is a major food source for local communities, and its numbers have been in decline since the late 1980s. The reason for the decline is unknown, but is likely caused by changes in their natural environment resulting from climate warming (Griffith et al., 2002). Along their migration route from wintering grounds in the southern Yukon to calving grounds on the north shore of the Beaufort Sea, the caribou vary their diet according to season, nutritional requirements, and food availability (Thomson and McCourt, 1981). Lichen is the major wintering food of caribou, and changes in lichen abundance and availability related to vascular plant increase are thought to be major contributing factors to the herd's decreasing numbers (Cornelissen et al., 2001).

Vegetation changes caused by climate warming have been investigated in controlled warming experiments across the Arctic (Hollister et al., 2005; Walker et al., 2006). Experimental warming has consistently produced an increase in vascular plant growth and a decrease in lichen and bryophyte abundance (Potter et al., 1995; Callaghan et al., 1999; Cornelissen et al., 2001; Dormann and Woodin, 2002; Gough and Hobbie, 2003; Van Wijk et al., 2003; Walker et al., 2006). These experiments support anecdotal evidence of overall greening in the North and observational evidence obtained through satellite observation (Myneni et al., 1997; Silapaswan et al., 2001; Zhou et al., 2001; Jia et al., 2003; Stow et al., 2003; Pouliot et al., in press) and repeat landscape photography (Sturm et al., 2001; Tape et al., 2006). Short- and long-term effects of warming on northern vegetation have been examined in Hollister et al. (2005). They suggest that initial and secondary responses are different: an alteration in growth and biomass allocation of previously established individuals occurs in the short term, while the long-term response is the result of integrated short-term responses in addition to changes in recruitment.

Vegetation monitoring using remote sensing data has generally employed the Normalized Difference Vegetation Index (NDVI) as a proxy for gross photosynthesis at broad spatial scales (Goetz et al., 2005). The NDVI exploits the contrast between red and near infrared reflectance (NIR) of vegetation, since chlorophyll is a strong absorber of red light, while the internal structure of leaves reflects highly in the NIR (Nemani and Running, 1989). The difference is normalized by the sum of the two bands to help compensate for changing illumination conditions, surface slope, aspect, and other extraneous factors. The NDVI ((NIR – Red)/(NIR + Red)) varies from –1 to +1. Clouds, water, and snow with more visible reflectance than near-infrared reflectance, generally have negative NDVI values. Rock and soil have NDVI values near zero, and vegetation generally yields positive NDVI values, which approach +1 with increasing plant chlorophyll content or green biomass.

Previously, we had used the NDVI to examine the short-term effects of temperature on northern vegetation productivity from remotely sensed imagery (Olthof and Latifovic, 2007). This study builds on the previous one by investigating longer-term effects of widespread temperature increase in the Arctic by vegetation type. Other research has noted extensive increasing NDVI in northern environments, attributed primarily to shrub expansion and increased vascular biomass caused by a longer growing season and higher temperatures. With the exception of few studies (e.g., Bunn and Goetz, 2006), these effects have been examined across all northern vegetation types simultaneously because coarse resolution data (from 1 to 8 km AVHRR) were used and vegetation types were mixed within each pixel's footprint. We use medium-resolution (30 m) Landsat time-series data in two separate locations in Canada's eastern and western taiga-tundra transition to examine recent vegetation-specific responses to climate warming. In addition, we use 1 km AVHRR data to monitor changes (at 1 km spatial scale) over homogeneous land cover targets previously identified in Olthof and Latifovic (2007).

METHODS

LANDSAT Data

Satellite data time-series were acquired for World Referencing System (WRS) Path/Row 61/12 in the Northwest Territories (NWT), Canada, just east of the Mackenzie Delta and south of the Tuktoyaktuk Peninsula, and Path/Row 20/19, located in northern Quebec on the eastern shore of Hudson Bay (Fig. 1). Both scenes are in the forest–tree line transition, though more of scene 61/12 is below the tree line than scene 20/19 according to Timoney et al. (1992) and Payette (1983). Thus, according to long-term provincial and territorial fire polygon databases, scene 61/12 contains more forest and is subject to fire disturbance, whereas scene 20/19 contains more tundra and experiences minimal fire disturbance.

Selection of scenes close in anniversary dates minimizes the seasonal effects of phenology and makes the time series comparison valid. Vegetation phenology is rapid in the Arctic because of the short growing season. In addition, cloud cover is frequent over much of northern

FIG 1. Locations of Landsat scenes used in the current analysis overlain on the northern tree-line limit (Timoney et al., 1992; Payette, 1983). WRS scene 61/12 covers the tree-line transition zone in the Yukon, while WRS scene 20/19 lies mostly above the tree line in northern Quebec.

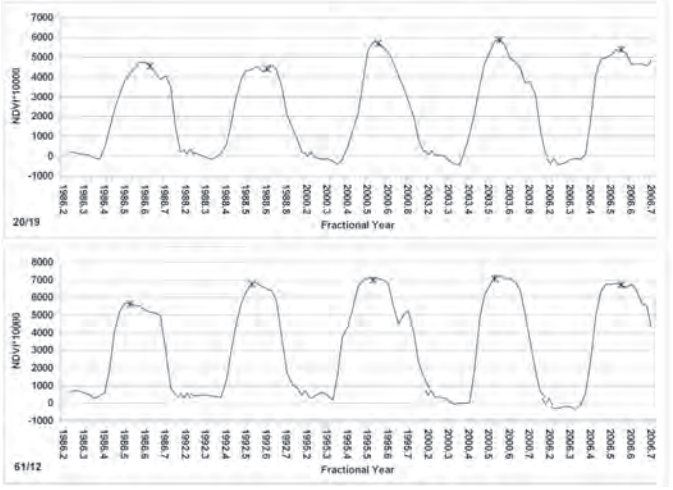

FIG. 2. Phenological timing of Landsat data used in each time series. Asterisks demark date of Landsat acquisition on seasonal 10-day AVHRR measurements for each year.

TABLE 1. Landsat scenes used for time-series analysis.

WRS Path/Row					
61/12 68.29° N, 131.46° W			20/19 58.71° N, 76.27° W		
Year	**Date**	**Sensor**	**Year**	**Date**	**Sensor**
1986	July 18	TM	1986	August 20	TM
1992	July 18	TM	1988	August 25	TM
1995	July 11	TM	2000	August 2	ETM+
2000	July 16	ETM+	2003	August 3	TM
2006	July 25	TM	2006	July 26	TM

Canada, reducing the availability of usable optical remote-sensing data. Landsat has a revisit time of 16 days. In a given year, therefore, no more than three acquisitions can occur within a month of an acquisition date anniversary from the previous year, and this number may be reduced at the beginning and end of the growing season. All of these factors make it difficult to obtain high-quality Landsat data for time-series analysis and are reasons why most analyses use coarse-resolution data with daily revisit times. Five mainly clear scenes from 1986 to 2006 were obtained for each area. Satellite data were acquired near the peak of the growing season (Fig. 2), within less than a month of anniversary dates for scene 20/19, and less than two weeks for 61/12, from TM and ETM+ sensors onboard Landsat 5 and 7 (Table 1).

Each time series was georeferenced to the 2000 ETM+ scene in each set (Fig. 3), which was obtained from the Centre for Topographic Information (CTI) orthoimage dataset created with the most accurate positional control data available at the time of creation (CTI, 2003). The images lacked manmade features, which are normally used for image-to-image registration, so lake centres, which are numerous and well dispersed in both images, were used as control points. With a minimum of 15 control points per image, this method produced RMS errors of less than 30 m, or one Landsat pixel. Because lakes have been disappearing in certain regions of the Arctic (Smith et al., 2005) and this phenomenon could be seen in the scenes that were analyzed, only lakes that appeared stable were used as targets. In any event, as long as lake bottoms are relatively symmetrical, lake centres should not migrate significantly with changing water levels.

Level 1G red and near-infrared bands required to calculate the NDVI were calibrated for Landsat 7 ETM+ using coefficients provided in the calibration file for conversion of scaled radiances to at-sensor radiances. Landsat 5 data were processed using the National Landsat Archive Production System (NLAPS) in March of 2007 using a Lookup Table (LUT) that was not up to date at the time the data were processed and analyzed for the current study. The recent Landsat 5 LUT released on 2 April 2007 was downloaded from the USGS Landsat project webpage (USGS, 2008) for use in calibration. Landsat 5 data were converted from scaled radiances to the previously released LUT radiance values using the coefficients provided in the header file. A ratio of the previously released LUT to the current LUT values was multiplied to update radiances to the new lifetime radiometric calibration curve (Equation 1, see Appendix). The full implementation of these processing changes led to an improved Landsat 5 TM data product that is more comparable to Landsat 7 Enhanced Thematic Mapper Plus (ETM+) radiometry, and provides the basis for long-term studies of the Earth's land surfaces (USGS, 2008). At-sensor radiance, sun elevation, band-specific solar irradiance values for Landsat 5 and 7, and earth-sun distance were used to convert at-sensor radiance to top-of-atmosphere reflectance.

Only clear-sky areas in all five scenes of each time series were analyzed. Clear sky was determined from a Haze Optimized Transform (HOT) (Zhang et al., 2002) mask generated for all haze- and cloud-contaminated

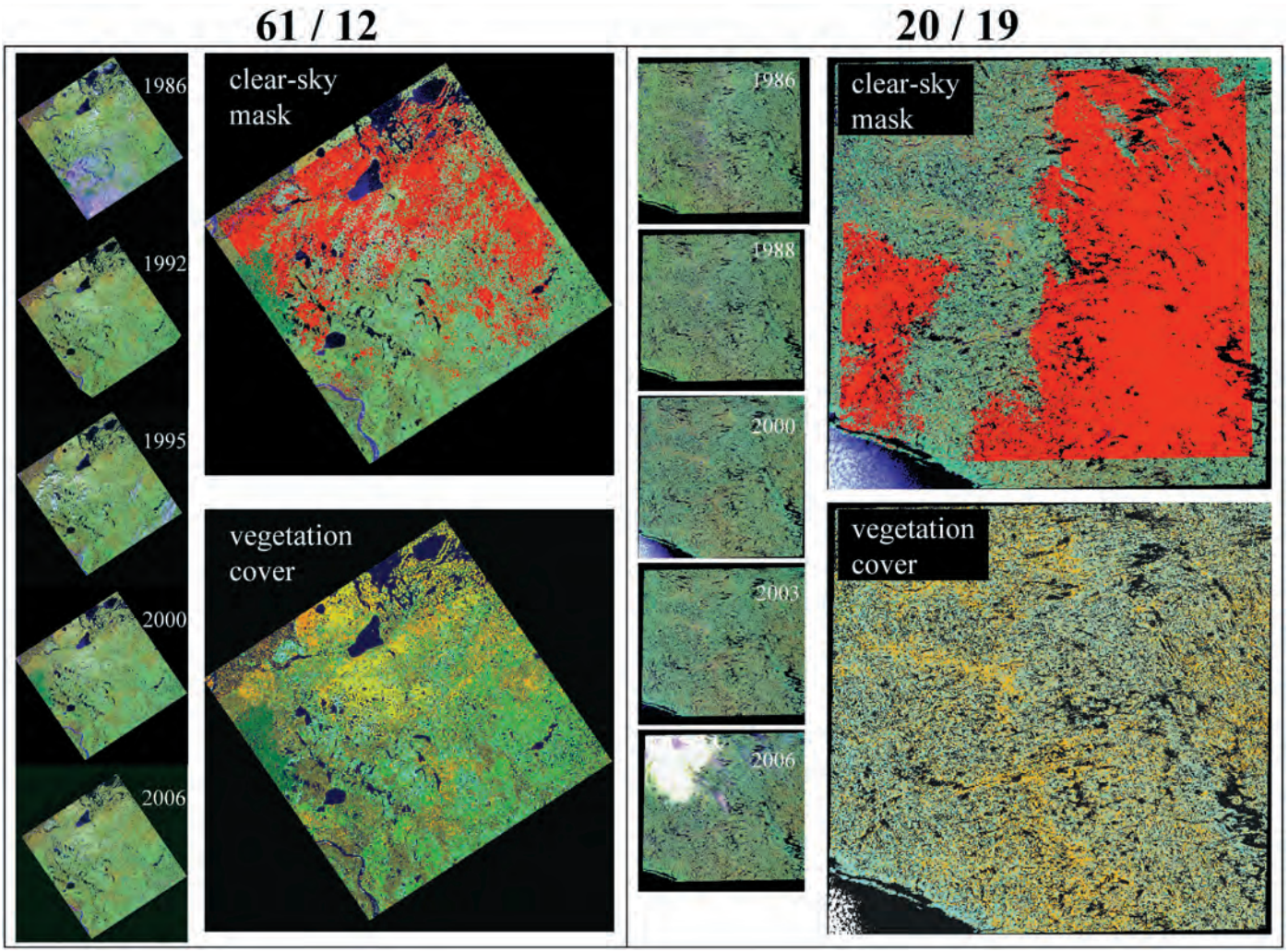

FIG. 3. Geometrically corrected and radiometrically calibrated Landsat time-series, with the vegetation community classification and intersection of clear-sky areas used for NDVI trend analysis.

images, and a conservatively low threshold was applied on each image's HOT mask to determine haze or cloudy areas. Intersection of clear-sky areas among all images in each set provided clear-sky areas for the time-series analysis. In addition, a NWT territorial fire polygon database was used to remove fire scars from scene 61/12 from 1965 onward to eliminate the effect of fire regeneration on NDVI trends.

AVHRR Data

Because seven lifetime calibration curves have been released for Landsat 5 since 2003, we wanted to check trends from the current calibration against another data source to ensure that any observed trends were not due to changes to the gain or offset in the lifetime calibration of the sensor. A 1 km AVHRR database recently developed for climate change studies over Canada (Latifovic et al., 2005) was used to monitor homogeneous 1 km land cover targets identified in Olthof and Latifovic (2007). AVHRR data were processed with an improved methodology for georeferencing and compositing (Latifovic et al., 2005), correction for viewing and illumination conditions (Latifovic et al., 2003), cloud screening (Khlopenkov and Trishchenko, 2006), and atmospheric correction. A full description of the processing system to top of atmosphere reflectance is provided in Latifovic et al. (2005). Atmospheric correction was performed using the Simplified Method for Atmospheric Correction (Rahman and Dedieu, 1994). Inputs included water vapour and pressure taken from the North America Regional Reanalysis Project (NCEP, 2007), ozone from the Total Ozone Mapping Spectrometer (NASA/GSFC, 2008), and stratospheric aerosol optical depth (AOD) at 550 nm from the Goddard Institute for Space Studies (GISS, 2007) (Pouliot et al., in press).

Land cover data used to identify homogenous AVHRR pixels was obtained from a 90 m Landsat coverage of northern Canada (Olthof et al., 2005) classified to 29 thematic classes based on the Federal Geographic Data Committee (FGDC) definitions (map and data are available on GeoGratis http://geogratis.cgdi.gc.ca/). The vegetative land cover types were merged to three dominant

TABLE 2. Lookup table to convert FGDC land cover classes in the Landsat land cover mosaic of northern Canada to dominant vegetation types: V = Vascular, L = Lichen, VL = Vascular/Lichen, NA = Not Applicable.

Code	FGDC Land Cover Class	Dominant Vegetation Type
1	Evergreen forest (> 75% cover)–old	V
3	Deciduous forest (> 75% cover)	V
4	Mixed coniferous (50–75% coniferous)–old	V
6	Mixed deciduous (25–50% coniferous)	V
7	Evergreen open canopy (40–60% cover)–moss-shrub understory	V
8	Evergreen open canopy (40–60% cover)–lichen-shrub understory	VL
9	Evergreen open canopy (25–40% cover)–shrub-moss understory	V
10	Evergreen open canopy (25–40% cover)–shrub-moss understory	V
13	Mixed evergreen-deciduous open canopy (25–60% cover)	V
14	Mixed deciduous (25–50% coniferous trees; 25–60% cover)	V
15	Low regenerating to young mixed cover	V
16	Deciduous shrubland (> 75% cover)	V
18	Herb-shrub-bare cover, mostly after perturbations	V
19	Open forest, shrub-herb-lichen-bare	V
20	Wetlands	V
21	Sparse coniferous (density 10–25%), shrub-herb-lichens cover	V
22	Sparse coniferous (density 10–25%), herb-shrub cover	V
23	Herb-shrub	V
24	Shrub-herb-lichen-bare	V
26	Lichen-shrubs-herb, bare soil or rock outcrop	L
28	Low vegetation cover (bare soil, rock outcrop)	NA
35	Lichen barren	L
36	Lichen-shrub-herb-bare	L
37	Sparse coniferous (density 10–25%), lichens-shrub-herb cover	VL
38	Rock outcrop, low vegetation cover	NA
39	Recent burns	NA
41	Low vegetation cover	NA
43	Water bodies	NA
45	Snow/ice	NA

types, Lichen, Vascular, and mixed Vascular/Lichen, for analysis (Table 2). For each land cover type, we calculated a 1 km homogeneity distribution based on the 90 m Landsat land cover. The samples within the highest 2% tail of the homogeneity distribution were retained for time-series analysis.

Landsat Vegetation Mapping

Landsat images WRS 61/12 and 20/19 for the year 2000 were classified to vegetation communities using the combined Enhancement Classification (Beaubien et al., 1999) and Classification by Progressive Generalization (Cihlar et al., 1998) methods (ECMCPG). Enhancement was performed by stretching ETM+ bands 4, 5, and 3 (displayed as red, green, and blue) to maximize the dynamic range occupied by land cover, while compressing water on the low end and cloud on the high end of the ranges. This step is performed to facilitate interpretation by maximizing the visible differences and improving the spectral separability among land cover types. Enhanced images were then clustered to 150 clusters using the unsupervised fuzzy k-means algorithm (Bezdek, 1973). A pseudo-colour table was generated from the cluster image that mimicked the colour of the enhanced imagery. At this and each subsequent generalization step, the generalized image with a new pseudo-colour table applied was compared visually to the previous one to ensure minimal loss of land cover information. Automatic cluster merging was performed on the basis of minimum Euclidean distance in a series of generalization steps until a 50–60 cluster image was obtained. From this point, manual merging was performed guided by field and other reference data.

Field data collected along the Dempster Highway in the summer of 2004 consisted of geolocated field photos, detailed descriptions of vegetation species abundance, and general land cover descriptions. Of the 137 sites surveyed, 14 were located within scene 61/12. To assist interpretation of vegetation cover, we used an Ikonos scene of the area surrounding Inuvik imaged on 25 July 2004, containing four spectral bands at 4 m resolution and a panchromatic band at 1 m resolution. We also used colour airphotos of the MacKenzie Valley (at 1:30000 scale, acquired in summer 2004) in interpreting the Landsat data (NWT Centre for Geomatics, 2008) and several high-resolution images available from Google Earth to check and verify vegetation cover.

For scene 20/19, detailed forest-tundra descriptions along the tree-line gradient, and specifically located near identifiable lakes in northern Quebec, as well as ground and oblique airphotos provided in Payette (1983), assisted interpretation. A paper by Petzold and Mulhern (1987) on vegetation gradients on slopes in the eastern Canadian Subarctic was also used, as were several high-resolution images in Google Earth. While some of these reference data were out of date, wholesale changes in vegetation communities are unlikely to have occurred since their acquisition. Also, some of the reference data were not precisely geolocated, and were therefore used to interpret topographic and latitudinal vegetation gradients rather than to assign specific labels at precise locations. Previous experience interpreting land cover was also relied on to guide vegetation community labeling. For scene 61/12, seven vegetation communities were found and described, while for scene 20/19, only four communities were described according to dominant plant functional types. Communities were then merged to the same dominant types used in the AVHRR analysis, i.e., Lichen, Vascular, and mixed Vascular/Lichen.

The lichen-dominated vegetation type contains other non-vascular vegetation types such as bryophytes, however, we use the term “lichen” to correspond to both lichen and other non-vascular plant types for convenience, since lichens comprise the majority of non-vascular cover in the two Landsat scenes. We recognize that lichens are not the only vegetation type in lichen-dominated regions; rather, they are often mixed with bare ground, vascular plants, and other non-vascular plants such as mosses. On our field campaigns in the Yukon, we have sampled areas with lichen

coverage greater than 70% at the scale of one 30 m Landsat pixel, while Petzold and Mulhern (1987) have noted greater than 90% lichen coverage in the region of scene 20/19 at 1 m^2 scale, and Theau and Duguay (2004) have also sampled areas in northern Quebec west of 20/19 with greater than 90% lichen within a mean area of 0.19 km^2. These lichen-dominated regions are composed primarily of bright lichens such as *Cladonia* and *Cladina* (reindeer moss) and are interpreted by their high reflectance in the three Landsat bands used for vegetation classification.

NDVI Trend Analysis

A robust regression technique called Thiel-Sen (Fernandes and Leblanc, 2005) was used to determine NDVI trends for clear sky areas over both Landsat scenes and AVHRR from 1986 to 2006. Mean NDVI was first calculated beneath each vegetation type and time period separately for each Landsat scene and peak annual AVHRR data. Thiel-Sen regression was then fit to the time-series of mean NDVI values. Thiel-Sen is a rank-based regression technique in which the slope is calculated from a series of cases with n independent and dependent observations as the median of all possible $(n \times (n\text{-}1)/2)$ pair-wise slopes. In effect, its slope calculation amounts to a statistical bootstrapping by considering all possible pair-wise observations at all time-lags. Because the Thiel-Sen slope is based on the median rank of all pair-wise slopes, it has been shown to be resistant to up to 29% outliers. The significance (p-values) of the rank-based correlation coefficient tau, which is a measure of the strength of the monotonic relationship between x and y, was computed for each regression line. The small sample approximation suitable for n of 10 or less was used to calculate p-values for Landsat regressions with $n = 5$ dates, while the large sample test statistic based on a standard normal distribution was used for AVHRR data where $n = 21$ (Kendall and Stuart, 1967).

Vegetation Change Simulations

In a separate analysis, forward linear spectral mixture analysis (Adams et al., 1986) was used to determine the likely nature of vegetation changes by simulating a range of possible vegetation changes that could produce the observed NDVI trends in Landsat and AVHRR. Linear mixture analysis is based on the energy conservation law, which proposes that a pixel's spectral response can be represented by the linear combination of areal fractions of pure endmember spectral signatures within the pixel footprint (Drake et al., 1999). Pure reference spectral signatures are referred to as endmembers (EM) because they represent the case where 100% of the sensor's field of view is occupied by a single cover type (Lillesand and Kiefer, 2000). Normally, spectral mixture analysis is used to unmix a signal to derive a single set of endmember fractions, whereas in the current case, we simulated an array of potential vegetation endmember fraction changes that could have led to the NDVI changes seen in satellite imagery. In addition, we simulated changes in the endmembers themselves to account for changes in endmember productivity due to altered climate conditions.

A three endmember model, consisting of lichen, vascular, and bare fraction endmembers was used, with NDVI endmember signatures extracted from peak-of-season NDVI values published in Olthof and Latifovic (2007) for three FGDC classes: 35, Lichen barren, representing the lichen endmember; 28, Low vegetation cover (bare soil, rock outcrop), representing bare; and 23, Herb-shrub, representing vascular. These endmembers were sampled from SPOT VGT surface reflectance under 1 km homogeneous patches across northern Canada within a range of productivity and endmember variability. Fractional change of each endmember varied from minus 2.3% to plus 2.3% in 0.1% increments based on extreme annual percent cover changes observed by Hollister et al. (2005) at the Barrow, Alaska experimental warming site. Endmembers were varied from -1 to +1 standard deviation (SD) in increments of 1 SD to account for endmember variability due to changes in endmember productivity. Equation 2 (see Appendix) was used to solve numerically for changes in lichen, bare, and vascular fractions and endmember signatures that approximate observed NDVI trends to within $\pm 10 \times 10^{-4}$ NDVI per year, with the additional constraint that the sum of changes in all three endmembers must equal zero. This additional constraint ensured that an increase in one endmember was accompanied by an equal decrease in the other two so that the total area remained constant.

RESULTS

Overall Trends

The average overall NDVI trends for scene 61/12 across all vegetation community types beneath the clear-sky area mask are presented in Table 3, along with other published values for the North Slope of Alaska and northern Yukon/NWT. While the region of northern NWT, Yukon, and Alaska that includes scene 61/12 has been studied extensively, no studies were found publishing specific NDVI trend values over northern Quebec.

Other published values represent slightly different regions, time periods, processing methods, and trend extraction techniques and therefore, differences exist among them. Stow et al. (2003) used Seasonally Integrated NDVI (SINDVI) calculated as the sum of bi-weekly NDVI values greater than 0.1 from April to October. In order to convert these values to single NDVI values, we assumed that all 14 bi-weekly time periods were valid; therefore, SINDVI values were divided by 14 to obtain annual growing season NDVI values representing the average two-week composite NDVI value from April to October. Had fewer composites met the minimum NDVI criterion,

TABLE 3. NDVI trend under clear-sky areas for Landsat WRS scene 61/12 and other published NDVI trend values for similar regions from AVHRR.

Author	Location	Years	Data	Comments	Range of delta NDVI per Year × 10 000
Current study	WRS 61/12	1986–2006	Landsat TM and ETM+	Calibrated	86
Zhou et al., 2001	Northern Hemisphere	1981–99	AVHRR GIMMs 8 km	Analyzed only vegetated pixels	28
Stow et al., 2003	North Slope of Alaska	1990–99	AVHRR 1 km GIMMS-corrected	Bi-weekly SINDVI from April to October	43–71
Jia et al., 2003	North Slope of Alaska	1981–2001	AVHRR GIMMs 8 km		28–41
Jia et al., 2003	North Slope of Alaska	1990–2000	AVHRR 1 km		39–66
Pouliot et al. (in press)	Canada	1985–2006	AVHRR 1 km		60

TABLE 4. NDVI × 10^{-4} trends by vegetation community for two Landsat scenes and corresponding dominant vegetation type.

	Landsat WRS Scene				Dominant
	61/12		20/19		Vegetation
	Slope	*p*	Slope	*p*	Type
Lichen barren	51.19	0.017	40.23	0.234	L
Lichen heath	68.58	0.017	45.99	0.484	L
Lichen/shrub	66.51	0.017			VL
Sparse conifer/shrub/lichen	82.20	0.084	50.51	0.484	VL
All clear sky	82.84	0.084	46.46	0.484	
Open conifer/shrub/moss	86.14	0.084			V
Herb/shrub	95.85	0.084	52.04	0.484	V
Broadleaf tree/shrub	101.60	0.084			V

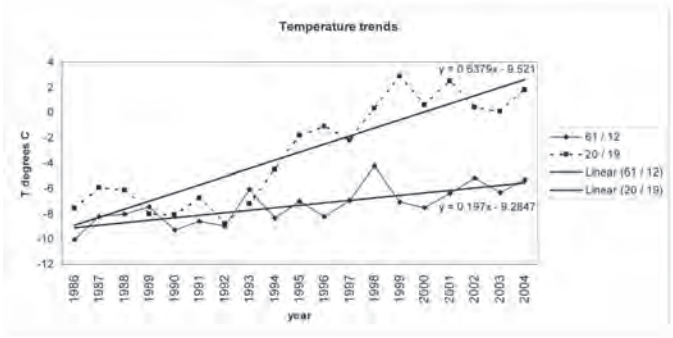

FIG. 4. 1986–2004 temperature trends for meteorological stations located in the vicinity of Landsat scene 20/19 (Inukjuak, northern Quebec, 58.46° N, 78.08° W) and scene 61/12 (Inuvik, Yukon, 68.31° N, 133.51° W).

values reported here for Stow et al. (2003) would have been higher. In addition, had only peak values met the criterion, the average would have also represented higher NDVI values.

Trends determined from Landsat data in the current study are higher than those obtained from other studies using AVHRR data. Regardless of differences among studies in terms of absolute NDVI trends, however, there is consensus in the direction of the NDVI trend for this region. This consensus among satellite observations is also supported by in-situ observational evidence of an overall greening of the North and specifically of anecdotal evidence suggesting increased shrubbiness in Alaska (Serreze et al., 2000; Sturm et al., 2001; Tape et al., 2006).

Both Landsat scenes exhibited positive overall NDVI trends, with scene 61/12 displaying a greater annual NDVI increase beneath the clear sky mask than scene 20/19 (Table 4). Both regions have exhibited significant warming, with the northern Quebec region of scene 20/19 having experienced greater annual and summer warming in the 1986–2004 period than the northern NWT region of scene 61/12 (Environment Canada, 2005) (Fig. 4).

Vegetation Community-Specific Trends

An examination of NDVI trends by dominant vegetation type reveals clear and consistent differences among them for both Landsat scenes (Table 4, Fig. 5). For both Landsat time series, vegetation communities with lichen have a much smaller annual NDVI increase than those dominated by vascular vegetation. The 2000 ETM+ data acquired from Landsat 7 appear to be biased towards higher NDVI values than those from Landsat 5, which were used for all other dates in both time series. In addition, the difference between high and low NDVI values is greater for Landsat 7 than for Landsat 5. This suggests a bias in the gain of Landsat 7 data compared to Landsat 5 for either the red or NIR channels used to calculate NDVI. Although calibration using the new lifetime curve for Landsat 5 should make Landsat 5 and 7 more comparable, others have identified a similar NDVI bias between sensors due to differences in the spectral response functions (Steven et al., 2003). This artifact, which is due to sub-optimal inter-sensor calibration, has likely had little effect on dominant vegetation type trend magnitude or on differences among trends for different vegetation types because of the robust regression method used, which is insensitive to 29% outliers (Fernandes and Leblanc, 2005).

Trends were significant at the 90th percentile in all cases for scene 61/12; however, trends in scene 20/19 were consistently insignificant at this level. This result is due to the previously mentioned sub-optimal inter-sensor calibration between Landsat 5 and 7 and the fact that the positively biased Landsat 7 scene was in the middle of the time series. Thus, all slopes from the Landsat 7 scene onward, or two of a possible 10 pair-wise slopes, were negative. These negative slopes had little impact on the trend magnitude, which was calculated from the median of all pair-wise slopes, but they had a more substantial effect on significance, which relies on the number of positive and negative slopes in the set of possible pair-wise slopes.

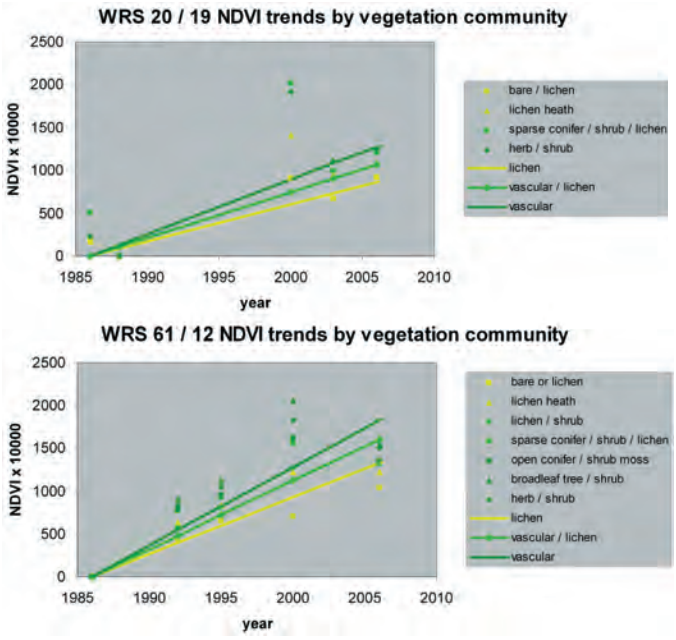

FIG. 5. 1986–2006 NDVI anomalies relative to 1986 by vegetation community type, and overall NDVI trends by dominant vegetation type for both Landsat scenes used in the analysis.

When spatially uniform vegetation types are collapsed to the three dominant vegetation types in the current analysis and monitored over select targets using AVHRR data, similar relative trends emerge, with vascular dominated communities exhibiting the greatest annual NDVI increase, lichen exhibiting the smallest annual NDVI increase, and mixed vascular/lichen showing an intermediate NDVI increase (Fig. 6). The magnitude of the absolute trends differs between Landsat and AVHRR data because of the greater variety of land cover samples included in the AVHRR analysis, merging of land cover to dominant vegetation types, and different scales and location of samples. However, regardless of the dataset used, the relative differences among vegetation types remain, with lichen-covered areas consistently exhibiting lower NDVI trends than vascular vegetation types (Table 5).

While absolute NDVI trends are different among dominant vegetation types, relative trends are similar when expressed as a percent increase from predicted 1986 NDVI. Thus, differences among absolute NDVI trends are normalized across vegetation types by the initial 1986 NDVI value. Because NDVI is related to biomass or productivity, this suggests that in general, a higher initial biomass produces a greater NDVI increase, and vice versa. Small discrepancies in the magnitude difference of relative NDVI change among vegetation types exist for the two regions examined, though these may reflect differences in climatic conditions. The AVHRR analysis suggests that while regional differences may exist, differences among vegetation types are small over all of northern Canada.

Both the Landsat and AVHRR-based trends suggest that all vegetation communities are greening and that vascular vegetation is greening more rapidly than lichen.

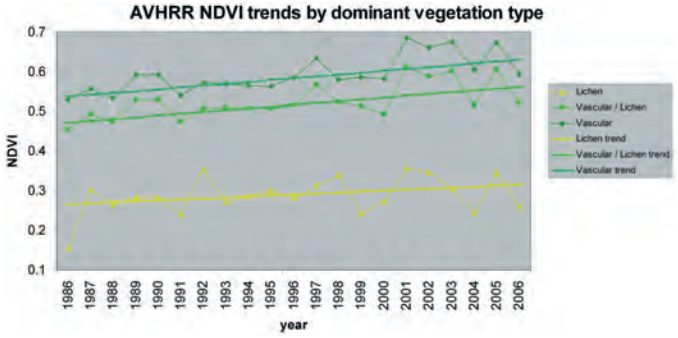

FIG. 6. 1986–2006 NDVI trends by dominant vegetation type from AVHRR.

The overall trend for all vegetation types beneath clear-sky areas can be used as a reference to assess the trends of different vegetation types. Other published NDVI trend values are all lower than the overall trend obtained from Landsat. Assuming the overall trend of all vegetation communities beneath clear-sky areas is 60×10^{-4} NDVI per year, which approximates the mean of other published values and represents the value obtained in Pouliot et al. (in press) from AVHRR over both Landsat scenes and the time period used in the current analysis, Landsat data still exhibit increasing NDVI trends across all vegetation communities and both scenes (Table 6).

Vegetation Change Simulations

Vegetation changes were simulated for the overall observed trend of 60×10^{-4} NDVI per year, as well as the 61/12 bias adjusted to AVHRR trend for the lichen/barren community of 30×10^{-4} NDVI per year as an extreme case. The simulated overall trend produced 4307 different possible changes in endmember fractions and signatures that approximate the observed trend of 60×10^{-4} NDVI per year, while the bare or lichen community trend was simulated using 6678 possible combinations of endmember changes. Figure 7 shows the frequency distribution of changes in lichen, bare, and vascular endmembers for two levels of NDVI change.

In order to produce the observed trend of 60×10^{-4} NDVI per year, the vascular fraction must increase by 0.7% per year or more, regardless of changes in endmember signatures due to productivity. If lichen is declining as the literature suggests, then the minimum vascular increase needed to produce the overall NDVI trend rises to more than 1.3% per year. Of the 6678 simulations that satisfied the conditions necessary to produce the observed NDVI trend of 30×10^{-4} NDVI per year, 6582, or 98.6% suggest that this trend is possible only given a vascular increase. Fifty-seven (0.9%) scenarios are possible without any changes in the vascular fraction, while a decrease in the vascular fraction can occur according to 39 (0.6%) simulations only if the lichen fraction increases by more than 1.8% and the lichen endmember signature increases by one standard deviation, or if the lichen fraction increases

TABLE 5. Average absolute NDVI $\times 10^{-4}$ trends and percent change from 1986 to 2006 by dominant vegetation type for two Landsat scenes and AVHRR.

	Landsat WRS Scene						AVHRR		
	61/12			20/19					
Dominant Vegetation Type	Slope	*p*	% Change	Slope	*p*	% Change	Slope	*p*	% Change
Lichen	66.51	0.017	28.0%	48.04	0.484	27.8%	24.45	0.227	18.4%
Vascular/Lichen	80.12	0.084	33.1%	50.51	0.484	27.1%	45.37	0.001	19.3%
Vascular	91.36	0.084	36.0%	52.04	0.484	24.2%	46.21	0.005	17.2%

TABLE 6. NDVI $\times 10^{-4}$ trends by vegetation community, bias adjusted to match NDVI trends from published long-term AVHRR studies in Table 3.

	WRS 61/12		WRS 20/19	
	Radiometrically Calibrated	Bias Adjusted to AVHRR Trend	Radiometrically Calibrated	Bias Adjusted to AVHRR Trend
Lichen barren	51.19	28.35	40.23	53.77
Lichen heath	68.58	45.74	45.99	59.53
Lichen/shrub	66.51	43.76		
Sparse conifer/shrub/lichen	82.20	59.36	50.51	64.05
All clear sky	82.84	60	46.46	60
Open conifer/shrub/moss	86.14	63.30		
Herb/shrub	95.85	73.01	52.04	65.58
Broadleaf tree/shrub	101.60	78.76		

by more than 2.1% and the endmember signature either remains constant or increases. These results suggest that changes in lichen or bare endmembers alone or in combination are not sufficient to produce the observed NDVI trends, and that in order for NDVI to have increased by 30×10^{-4} NDVI per year or more, vascular vegetation is almost certainly increasing in all communities.

DISCUSSION AND CONCLUSION

Short- and longer-term response of NDVI by vegetation type obtained from satellite observations and supported by controlled experiments suggests changes in northern vegetation and greening of all vegetation types, but at different rates. An overall greening trend has been attributed to increased shrubbiness and vascular plant growth, both of which have contributed to lichen decline through the effect of competition. Thus, vascular and shrub vegetation cover is increasing in biomass, while lichen-covered areas in the low Arctic are experiencing a transition from lichen to vascular cover (Cornelissen et al., 2001).

In the short term, experimental evidence suggests that acclimation of lichens to changing environmental conditions is rapid and has been shown to occur in a matter of days. Increased temperature in the absence of limiting moisture causes increased lichen photosynthesis to temperature levels seldom reached in the Arctic (Carstairs and Oechel, 1978). Therefore, with sufficient moisture, temperature by itself rarely causes a decrease in lichen productivity. However, the secondary effect of drying due to elevated temperature has a much more pronounced effect on lichen photosynthesis (Larson and Kershaw, 1975). A lack of sophisticated water supply and water retention mechanisms compared to higher plants makes lichens particularly sensitive to changes in moisture conditions. Under a wide range of temperature and light conditions, optimal water contents for photosynthesis were determined to be between 35% and 55% of saturation (Carstairs and Oechel, 1978).

The short-term effect of temperature on lichens has been shown to manifest itself in the NDVI signal of remotely sensed imagery. Using northern land cover from Landsat to identify homogeneous 1 km patches of vegetation and multi-temporal 1 km SPOT VGT data to monitor those areas through time, Olthof and Latifovic (2007) showed that unseasonably warm temperatures in the preceding month led to an increase in NDVI for land cover types occupied by vascular plants and suppressed NDVI over land cover types occupied by lichens and bryophytes. Carstairs and Oechel (1978) also found through controlled experimentation that the photosynthetic rate of lichens reflects the light and temperature conditions experienced during the month preceding the productivity measurement. This response in NDVI was observed only in humid areas of Canada, where precipitation exceeds potential evapotranspiration. These observations and controlled experimental warming evidence suggest that lichens adapted to relatively moist conditions are impaired through the secondary effect of temperature, which causes drying below the optimal water content determined by Carstairs and Oechel (1978).

In the medium to long term, experimental warming across the tundra biome has consistently shown lichen decline, which is primarily due to increased competition from vascular plants (Cornelissen et al., 2001). Hollister et

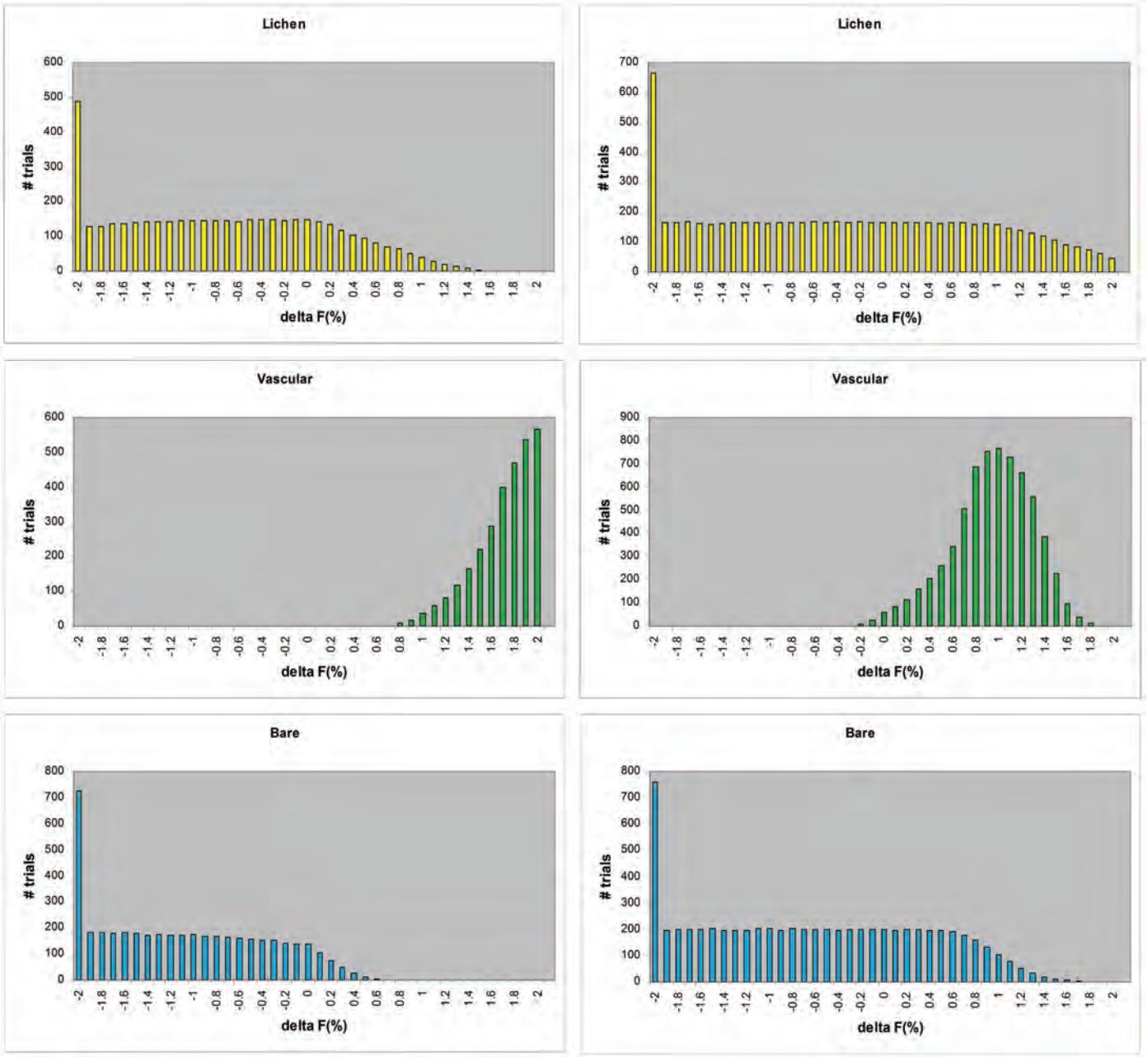

FIG. 7. Frequency distributions of simulated changes in lichen, vascular, and bare fractions accounting for variable endmember NDVI signatures, from linear spectral mixture analysis required to produce observed overall NDVI trends (60×10^{-4} – left) and bias-adjusted to AVHRR trends (30×10^{-4} – right).

al. (2005) proposed that the long-term effect was the result of numerous short-term physiological responses plus changes in recruitment. Thus, remote sensing and in-situ monitoring suggest that the medium- to longer-term effects of northern climate warming on lichen are likely caused by a combination of factors. First, increasing temperatures lead to drier conditions, producing suboptimal growth conditions for lichens particularly in humid northern regions. Prolonged drought may also favor vascular plants, as their developed root systems and water retention capabilities can cope better with limited moisture. Second, warmer temperatures lead to increased vascular plant growth via temperature fertilization and a lengthening of the growing season. And third, as vascular plants begin to occupy previously lichen-covered areas, they cast shade and further inhibit lichen productivity (Cornelissen et al., 2001).

The observed increase in NDVI for lichen-covered areas is likely due to increased recruitment of vascular plants and therefore represents a transition from lichen- to vascular-dominated vegetation associations. The short-term response of lichen NDVI decrease related to unseasonably warm temperatures in the preceding month suggests physiological impairment, which is likely the result of lichen desiccation from the secondary effect of temperature, rather than the result of temperature itself. Olthof and Latifovic (2007) suggested that in the longer term, lichen

abundance in the North may be the result of more frequent episodic warming that suppresses lichen productivity through drying. It seems likely that lichen decline is partly caused by impaired physiology, and that small longer-term NDVI increase over lichen-covered areas is partly due to lichen decline, which is more than offset by vascular plant increase, producing a net positive NDVI trend.

Similar NDVI increase relative to baseline NDVI across vegetation types was somewhat surprising because our analysis suggests different growth and successional processes occurring for each. In the case of vascular-dominated communities, NDVI increase may be attributed to differences in both physiology, which manifests itself in changes in leaf chemistry and reflectance, and plant morphology, which manifests itself as changes in biomass. For lichen-dominated communities, simulations suggest succession from lichen to vascular, possibly accompanied by changes in vascular leaf level reflectance. While processes are different between dominant vegetation types, similar relative trends suggest a common underlying process governing NDVI increase, such as site productivity. The fact that NDVI increase relative to baseline NDVI is fairly constant across vegetation types suggests that the magnitude of absolute NDVI may be predicted from baseline NDVI. However, the period over which NDVI increases are observed is relatively short. In time, biomass or productivity measured by NDVI will become limited by a factor other than temperature. Thus, while in the observed period we noted a direct relation between baseline NDVI and NDVI increase across vegetation types, this relation may not hold in the future when additional limiting factors to growth emerge.

Errors exist in both the Landsat-based land cover of northern Canada and in the two vegetation community maps generated for this analysis. Formal accuracy assessments were not conducted to evaluate the quality of these products. NDVI trends were determined for both Landsat scenes based on eight vegetation communities prior to merging to dominant vegetation types, while merging FGDC land cover classes to similar dominant vegetation types was done prior to analysis of trends in AVHRR data. While errors may exist at the level of eight vegetation communities in the case of Landsat time-series analysis, or 29 FGDC classes in the case of AVHRR, it is well known that mapping accuracy increases with decreasing thematic detail (Latifovic and Olthof, 2004) and therefore, classifications should be sufficiently accurate at the level of three dominant vegetation types to assess differences in trends.

The vegetation change simulation showed that vascular vegetation must be increasing in all communities in order to produce the observed NDVI trends, and experimental warming supports this finding. We allowed NDVI endmembers of lichen, bare, and vascular to vary within one standard deviation to account for changes in productivity. It should be noted that this range of endmember variation could account for observed changes in productivity on its own. However, endmember variation is due to both changes in endmember composition across space and changes in productivity in space and time, and these two factors cannot be examined separately. The large variation in the bare endmember is due primarily to different rock types sampled across the North, and other authors (e.g., Small, 2004) have noted that substrate is the most compositionally variable and least constrained endmember in mixing space. Both the lichen and bare endmember variation could easily account for observed NDVI trends, as they are within the range of approximately 0.3 to 0.6 of one SD for each of the two endmembers. Thus, a 100% vascular cover could produce the observed NDVI trends without any changes in vegetation composition simply though an increase in endmember productivity. It should be noted also that while endmember fractions are treated in two-dimensional space as a flat surface, they are three-dimensional entities that normally change in all three dimensions simultaneously. Therefore, an increase in cover is usually accompanied by an increase in volume, especially for plants with a vertical structure, and therefore we would normally expect a simultaneous change in cover and endmember reflectance. For this reason, canopy reflectance modeling that accounts for mutual shading of canopy objects might give a more exact simulation of northern vegetation changes.

Olthof and Latifovic (2007) showed that unseasonably warm temperatures in the preceding period suppressed lichen NDVI and enhanced vascular NDVI, and experimental warming suggests that this result may be due to the secondary effect of drying rather than the effect of temperature itself. Simulations showed that the observed trend of 30×10^{-4} NDVI per year was likely due to an increase in vascular vegetation, though a small possibility existed for a decrease in vascular and an increase in lichen if the lichen endmember signature was enhanced. Though the latter scenario is theoretically possible, experimental warming supported by findings in Olthof and Latifovic (2007) suggests that it is unlikely since both the amount of lichen and its NDVI tend to decrease with increased temperature. However, the interaction of temperature and moisture on plant competition and endmember variability is complex and has not been analyzed specifically in the current paper.

The simple three-endmember model could have included additional endmembers such as water and possibly bryophytes due to documented disappearance of Arctic lakes in Siberia and Alaska (Smith et al., 2004; Stow et al., 2004) and changes in hydrology due to permafrost melt. While these endmembers occur extensively in the North in combination with those analyzed, they were omitted for simplicity. Increasing NDVI is documented as widespread in the North (Pouliot et al., in press) and vast areas are occupied by only the three endmembers analyzed. In these regions, vascular vegetation increase must be prevalent according to our analysis.

In the current paper, we have analyzed two high quality Landsat time-series in different regions of Canada in

addition to select targets across northern Canada with AVHRR data, and all data have shown similar NDVI trends according to vegetation type. Thus, vegetation changes appear to be consistent between regions and among vegetation types. Lichen-dominated communities are greening at a much slower rate than vascular-dominated communities, and this phenomenon appears to be widespread in the North. The effects that these vegetation changes are having on wildlife and on communities dependent on hunting need to be investigated further.

ACKNOWLEDGEMENTS

The authors are grateful to Richard Fernandes, Robert Fraser, and three anonymous reviewers whose comments helped greatly improve this paper. The work is financially supported by the Canada International Polar Year initiative, through the project entitled "Climate Change Impacts on Canadian Arctic Tundra Ecosystems: Interdisciplinary and Multi-scale Assessments". We also received financial and administrative support from the Earth Science Sector, Natural Resources Canada, through the Enhancing Resilience to a Changing Climate program.

APPENDIX

Equation 1

$$L_{\lambda 8a} = G_{rescale} \times Q_{cal} + B_{rescale}$$

$$L_{\lambda 8a} = \frac{Q}{G8a}$$

$$\frac{L_{\lambda 8a} \times G8a}{G9a} = \frac{Q}{G9a} = L_{\lambda 9a}$$

where:

Q = raw quantized voltage or response [DN].
$G8a$ = detector gain or responsivity [DN/ (W/ (m^2 sr μm)] for previous LUT release.
$G9a$ = detector gain or responsivity [DN/ (W/ (m^2 sr μm)] for current LUT release.
$L_{\lambda 8a}$ = spectral radiance at the sensor's aperture [W/ (m^2 sr μm)] for previous LUT release.
$L_{\lambda 9a}$ = spectral radiance at the sensor's aperture [W/ (m^2 sr μm)] for current LUT release.
Q_{cal} = quantized calibrated pixel value [DN].
$G_{rescale}$ = band-specific rescaling gain factor [(W/ (m^2 sr μm))/ DN].
$B_{rescale}$ = band-specific rescaling bias factor [W/ (m^2 sr μm)].

Equation 2

Solve for percent change in lichen (ΔL), bare (ΔB), and vascular (ΔV) such that:

$$\overline{NDVI}_L \pm 1SD_L \times \Delta L + \overline{NDVI}_B \pm 1SD_B \times \Delta B + \overline{NDVI}_V \times \Delta V = \Delta NDVI \pm 10 \times 10^{-4}$$

$$\Delta L + \Delta B + \Delta V = 0$$

where $NDVI_L \pm 1SD_L$ = Lichen NDVI endmember ± one standard deviation = 0.289 ± 0.021, $NDVI_B \pm 1SD_B$ = Bare NDVI endmember ± one standard deviation = 0.228 ± 0.057, and $NDVI_V \pm 1SD_V$ = Vascular NDVI endmember ± one standard deviation = 0.563 ± 0.022 (Olthof and Latifovic, 2007).

REFERENCES

ACIA (ARCTIC CLIMATE IMPACT ASSESSMENT). 2004. Impacts of a warming Arctic. Cambridge: Cambridge University Press. http://www.acia.uaf.edu. 140 p.

ADAMS, J.B., SMITH, M.O., and JOHNSON, P.E. 1986. Spectral mixture modeling: A new analysis of rock and soil types at the Viking Lander 1 site. Journal of Geophysical Research 91: 8098–8112.

BEAUBIEN, J., CIHLAR, J., SIMARD, G., and LATIFOVIC, R. 1999. Land cover from multiple Thematic Mapper scenes using a new enhancement-classification methodology. Journal of Geophysical Research 104:27909–27920.

BEZDEK, J.C. 1973. Fuzzy mathematics in pattern classification. PhD dissertation, Cornell University, Ithaca, New York.

BUNN, A., and GOETZ, S. 2006. Trends in satellite-observed circumpolar photosynthetic activity from 1982 to 2003: The influence of seasonality, cover type, and vegetation density. Earth Interactions 10:1–19.

CALLAGHAN, T.V., PRESS, M.C., LEE, J.A., ROBINSON, D., and ANDERSON, C. 1999. Spatial and temporal variability in the responses of Arctic terrestrial ecosystems to environmental change. Polar Research 18:1–7.

CARSTAIRS, A.G., and OECHEL, W.C. 1978. Effects of several microclimatic factors and nutrients on net carbon dioxide exchange in *Cladonia alpestris* (L.) Rabh. in the Subarctic. Arctic and Alpine Research 10:81–94.

CIHLAR, J., and BEAUBIEN, J. 1998. Land cover of Canada, Version 1.1. Special Publication, NBIOME Project. Ottawa, Ontario: Canada Centre for Remote Sensing and the Canadian Forest Service, Natural Resources Canada.

CIHLAR, J., XIAO, Q., CHEN, J., BEAUBIEN, J., FUNG, K., and LATIFOVIC, R. 1998. Classification by progressive generalization: A new automated methodology for remote sensing multichannel data. International Journal of Remote Sensing 19:3141–3168.

CORNELISSEN, J.H.C., CALLAGHAN, T.V., ALATALO, J.M., MICHELSEN, A., GRAGLIA, E., HARTLEY, A.E., HIK, D.S., HOBBIE, S.E., PRESS, M.C., ROBINSON, C.H., HENRY, G.H.R., SHAVER, G.R., PHOENIX, G.K., JONES, D.G., JONASSON, S., CHAPIN, F.S., III, MOLAU, U., NEILL, C., LEE, J.A., MELILLO, J.M., SVEINBJÖRNSSON, B., and AERTS, R. 2001. Global change and Arctic ecosystems: Is

lichen decline a function of increases in vascular plant biomass? Journal of Ecology 89:984–994.

CTI (CENTRE FOR TOPOGRAPHIC INFORMATION). 2003. Landsat 7 orthorectified imagery over Canada, Level 1 product specifications, edition 1. Ottawa, Ontario: Natural Resources Canada Centre for Topographic Information.

DORMANN, C.F., and WOODIN, S.J. 2002. Climate change in the Arctic: Using plant functional types in a meta-analysis of field experiments. Functional Ecology 16:4–17.

DRAKE, N.A., MACKIN, S., and SETTLE, J.J. 1999. Mapping vegetation, soils, and geology in semiarid shrublands using spectral matching and mixture modeling of SWIR AVIRIS imagery. Remote Sensing of Environment 68:12–25.

ENVIRONMENT CANADA. 2005. Climate data CD-ROM (CDCD) – AES daily temp/precip data on CD-ROM – from 1880s up to present for Canadian stations. Ottawa: Environment Canada.

FERNANDES, R.A., and LEBLANC, S.G. 2005. Appropriate linear regression techniques for the calibration of remote sensing models: When classical linear regression should not be used. Remote Sensing of Environment 95:303–316.

GISS (GODDARD INSTITUTE FOR SPACE STUDIES). 2007. Forcings in GISS climate model: Stratospheric aerosol optical thickness. http://data.giss.nasa.gov/modelforce/strataer.

GOETZ, S.J., BUNN, A.G., FISKE, G.J., and HOUGHTON, R.A. 2005. Satellite-observed photosynthetic trends across boreal North America associated with climate and fire disturbance. Proceedings of the National Academy of Sciences 102: 13521–13525.

GOUGH, L., and HOBBIE, S.E. 2003. Responses of moist non-acidic Arctic tundra to altered environment: Productivity, biomass and species richness. Oikos 103:204–216.

GRIFFITH, B., DOUGLAS, D.C., WALSH, N.E., YOUNG, D.D., McCABE, T.R., RUSSELL, D.E., WHITE, R.G., CAMERON, R.D., and WHITTEN, K.R. 2002. The Porcupine caribou herd. In: Douglas, D.C., Reynolds, P.E., and Rhode, E.B., eds. Arctic Refuge coastal plain terrestrial wildlife research summaries. U.S. Geological Survey, Biological Resources Division, Biological Science Report USGS/BRD BSR-2002-0001:8–37.

HOLLISTER, R.D., WEBBER, P.J., and TWEEDIE, C.E. 2005. The response of Alaskan Arctic tundra to experimental warming: Differences between short- and long-term responses. Global Change Biology 11:525–536.

IPCC (INTERGOVERNMENTAL PANEL ON CLIMATE CHANGE). 2007. Climate change 2007: The physical science basis. Contribution of Working Group I to the Fourth Assessment Report of the Intergovernmental Panel on Climate Change. Solomon, S., Qin, D., Manning, M., Marquis, M., Averyt, K., Tignor, M.M.B., Miller, H.L., Jr., and Chen, Z., eds. Cambridge and New York: Cambridge University Press.

JIA, G.J., EPSTEIN, H.E., and WALKER, D.A. 2003. Greening of Arctic Alaska, 1981-2001. Geophysical Research Letters, 30(20), 2067, doi:10.1029/2003GL018268.

KENDALL, M.G., and STUART, A.S. 1967. Advanced theory of statistics, Vol. 2. London: Charles Griffin and Company.

KHLOPENKOV, K., and TRISHCHENKO, A. 2006. SPARC: New cloud, clear-sky, snow/ice and cloud shadow detection scheme for historical AVHHR 1-km observations over Canada. Journal of Atmospheric and Oceanic Technology 24:322–343.

LARSON, D.W., and KERSHAW, K.A. 1975. Acclimation in Arctic lichens. Nature 254:421–423.

LATIFOVIC, R., and OLTHOF, I. 2004. Accuracy assessment using sub-pixel fractional error matrices of global land cover products derived from satellite data. Remote Sensing of Environment 90:153–165.

LATIFOVIC, R., CIHLAR, J., and CHEN, J. 2003. A comparison of BRDF models for the normalization of satellite optical data to a standard sun-target-sensor geometry. IEEE Transactions on Geoscience and Remote Sensing 41(8):1889–1898.

LATIFOVIC, R., TRISHCHENKO, A.P., CHEN, J., PARK, W.B., KHOLPENKOV, K.V., FERNANDES, R., POULIOT, D., UNGUREANU, C., LUO, Y., WANG, S., DAVIDSON, A., and CIHLAR, J. 2005. Generating historical AVHRR 1 km baseline satellite data records over Canada suitable for climate change studies. Canadian Journal of Remote Sensing 31:324–346.

LILLESAND, T.M., and KIEFER, R.W. 2000. Remote sensing and image interpretation, 4th ed. New York: John Wiley & Sons, Inc.

MYNENI, R.B., KEELING, C.D., TUCKER, C.J., ASRAR, G., and NEMANI, R.R. 1997. Increased plant growth in the northern high latitudes from 1981–1991. Nature 386:698 –702.

NASA/GSFC (NATIONAL AERONAUTICS AND SPACE ADMINISTRATION/GODDARD SPACE FLIGHT CENTER). 2008. Total ozone mapping spectrometer. http://toms.gsfc.nasa.gov/ozone/ozone_v8.html.

NCEP (NATIONAL CENTERS FOR ENVIRONMENTAL PREDICTION). 2007. North American Regional Reanalysis homepage. http://www.emc.ncep.noaa.gov/mmb/rreanl/.

NEMANI, R.R., and RUNNING, S.W. 1989. Estimation of regional surface resistance to evapotranspiration from NDVI and thermal-IR AVHRR data. Journal of Applied Meteorology 28:276–284.

NWT CENTRE FOR GEOMATICS. 2008. Mackenzie Valley Air Photo Project. http://www.gnwtgeomatics.nt.ca/RemoteSensing/avhrr/MackenzieValleyPhotos.asp.

OLTHOF, I., and LATIFOVIC, R. 2007. Short-term response of Arctic vegetation NDVI to temperature anomalies. International Journal of Remote Sensing 28:4823–4840.

OLTHOF, I., BUTSON, C., FERNANDES, R., FRASER, R., LATIFOVIC, R., and ORAZIETTI, J. 2005. Landsat ETM+ mosaic of northern Canada. Canadian Journal of Remote Sensing 31:412–419.

PAYETTE, S. 1983. The forest-tundra and present tree-lines of the northern Quebec-Labrador peninsula. In: Morisset, P., and Payette, S., eds. International Conference on Tree-Line Ecology: Proceedings of the Northern Quebec Treeline Conference, 22 June–1 July 1981, Kuujjuarapik, Quebec, Canada. Nordicana 47:3–23.

PETZOLD, D.E., and MULHERN, T. 1987. Vegetation distributions along lichen-dominated slopes of opposing aspect in the eastern Canadian Subarctic. Arctic 40(3):221–224.

POTTER, J.A., PRESS, M.C., CALLAGHAN, T.V., and LEE, J.A. 1995. Growth responses of *Polytrichum commune* Hedw. and *Hylocomium splendens* (Hedw.) Br. Eur. to simulated environmental change. New Phytologist 131:533–541.

POULIOT, D., LATIFOVIC, R., and OLTHOF, I. In press. Detection and evaluation of NDVI trends in Canada from 1985–2006. International Journal of Remote Sensing.

RAHMAN, H., and DEDIEU, G. 1994. SMAC: A simplified method for the atmospheric correction of satellite measurements in the solar spectrum. International Journal of Remote Sensing 15:123–143.

SERREZE, M.C., WALSH, J.E., CHAPIN, F.S., III, OSTERKAMP, T., DYURGEROV, M., ROMANOVSKY, V., OECHEL, W.C., MORISON, J., ZHANG, T., and BARRY, R.G. 2000. Observational evidence of recent change in the northern high-latitude environment. Climatic Change 46:159–207.

SILAPASWAN, C.S., VERBYLA, D.L., and McGUIRE, A.D. 2001. Land cover change on the Seward Peninsula: The use of remote sensing to evaluate the potential influences of climate warming on historical vegetation dynamics. Canadian Journal of Remote Sensing 27(5):542–554.

SMALL, C. 2004. The Landsat ETM+ spectral mixing space. Remote Sensing of Environment 93:1–17.

SMITH, L.C., SHENG, Y., MACDONALD, G.M., and HINZMAN, L.D. 2005. Disappearing Arctic lakes. Science 308:1429.

STEVEN, M.D., MALTHUS, T.J., BARET, F., XU, H., and CHOPPING, M.J. 2003. Intercalibration of vegetation indices from different sensor systems. Remote Sensing of Environment 88:412–422.

STOW, D.A., DAESCHNER, S., HOPE, A., DOUGLAS, D., PETERSEN, A., MYNENI, R., ZHOU, L., and OECHEL, W. 2003. Variability of the seasonally integrated normalized difference vegetation index across the North Slope of Alaska in the 1990s. International Journal of Remote Sensing 24: 1111–1117.

STOW, D.A., HOPE, A., McGUIRE, D., VERBYLA, D., GAMON, J., HUEMMRICH, F., HOUSTON, S., RACINE, C., STURM, M., TAPE, K., HINZMAN, L., YOSHIKAWA, K., TWEEDIE, C., NOYLE, B., SILAPSWAN, C., DOUGLAS, D., GRIFFITH, B., JIA, G., EPSTEIN, H., WALKER, D., DAESCHNER, S., PETERSEN, A., ZHOU, L., and MYNENI, R. 2004. Remote sensing of vegetation and land-cover change in Arctic tundra ecosystems. Remote Sensing of Environment 89:281–308.

STURM, M., RACINE, C., and TAPE, K. 2001. Increasing shrub abundance in the Arctic. Nature 411:546–547.

TAPE, K., STURM, M., and RACINE, C. 2006. The evidence for shrub expansion in northern Alaska and the Pan-Arctic. Global Change Biology 12:686–702, doi: 10.1111/j.1365-2486.2006.01128.x.

THEAU, J., and DUGUAY, C.R. 2004. Lichen mapping in the summer range of the George River caribou herd using Landsat TM imagery. Canadian Journal of Remote Sensing 30: 867–881.

THOMSON, D.C., and McCOURT, K.H. 1981. Seasonal diets of the Porcupine caribou herd. American Midland Naturalist 105:70–76.

TIMONEY, K.P., LA ROI, G.H., ZOLTAI, S.C., and ROBINSON, A.G. 1992. The High Subarctic forest-tundra of northwestern Canada: Position, width, and vegetation gradients in relation to climate. Arctic 45(1):1–9.

USGS (U.S. GEOLOGICAL SURVEY). 2008. Landsat 5 Thematic Mapper (TM) calibration files. http://landsat.usgs.gov/science_L5_cpf.php.

VAN WIJK, M.T., CLEMMENSEN, K.E., SHAVER, G.R., WILLIAMS, M., CALLAGHAN, T.V., CHAPIN, F.S., III, CORNELISSEN, J.H.C., GOUGH, L., HOBBIE, S.E., JONASSON, S., LEE, J.A., MICHELSEN, A., PRESS, M.C., RICHARDSON, S.J., and RUETH, H. 2003. Long-term ecosystem level experiments at Toolik Lake, Alaska, and at Abisko, northern Sweden: Generalizations and differences in ecosystem and plant type responses to global change. Global Change Biology 10:105–123.

WALKER, M.D., WAHREN, C.H., HOLLISTER, R.D., HENRY, G.H.R, AHLQUIST, L.E., ALATALO, J.M., BRET-HARTE, M.S., CALEF, M.P., CALLAGHAN, T.V., CARROLL, A.B., EPSTEIN, H.E., JÓNSDÓTTIR, I.S., KLEIN, J.A., MAGNÚSSON, B., MOLAU, U., OBERBAUER, S.F., REWA, S.P., ROBINSON, C.H., SHAVER, G.R., SUDING, K.N., THOMPSON, C.C., TOLVANEN, A., TOTLAND, Ø., TURNER, P.L., TWEEDIE, C.E., WEBBER, P.J., and WOOKEY, P.A. 2006. Plant community responses to experimental warming across the tundra biome. Proceedings of the National Academy of Sciences 103:1342–1346, doi: 10.1073/pnas.0503198103.

ZHANG, Y., GUINDON, B., and CIHLAR, J. 2002. An image transform to characterize and compensate for spatial variations in thin cloud contamination of Landsat images. Remote Sensing of Environment 82:173–187.

ZHOU, L., TUCKER, C.J., KAUFMANN, R.K., SLAYBACK, D., SHABANOV, N.V., and MYNENI, R.B. 2001. Variations in northern vegetation activity inferred from satellite data of vegetation index during 1981 to 1999. Journal of Geophysical Research 106(D17):20069–20083.